


 Cite this: *RSC Adv.*, 2022, **12**, 26106

Received 14th June 2022
 Accepted 3rd September 2022
 DOI: 10.1039/d2ra03668a
rsc.li/rsc-advances

Ratiometric rapid distinction of two structurally similar fluoroquinolone antibiotics by a Tb/Eu hydrogel†

 Ananya Biswas and Uday Maitra  *

Norfloxacin and ofloxacin are two frequently prescribed second-generation fluoroquinolone antibiotics with an identical 4-quinolone chromophore and hence, are difficult to distinguish by conventional methods (UV or fluorescence). We have designed a $\text{Tb}^{3+}/\text{Eu}^{3+}$ /cholate cocktail that enabled us to differentiate these two drugs and rapidly measure their concentrations when present together. Additionally, a Tb^{3+} -cholate gel-based paper sensor was developed to detect and quantify them in a single drug containing system with a limit of detection (LOD) well below 100 nM.

Fluoroquinolone antibiotics belong to one of the most important classes of human and veterinary medicines owing to their broad-spectrum activity and effective oral absorption. Norfloxacin and ofloxacin (Fig. 1) are among the most prescribed second generation fluoroquinolone antibiotics^{1,2} used for the treatment of respiratory and urinary tract infections, ocular and skin infections, pelvic inflammatory disease, gonococcal urethritis, infectious diarrhoea, *etc.* However, potential adverse reactions such as tendinitis, tendon rupture, arthralgia, myalgia, peripheral neuropathy, hematuria, and central nervous system effects due to their excess intake have been well documented in the literature.³ Extensive use and misuse of the antibiotics as veterinary medicines have led to their appearance in milk,^{4,5} chicken⁶ and fish⁷ imposing adverse side effects for the consumer. Contamination of municipal wastewater, surface water and even groundwater results from their extensive usage, and from their excretion from human and animals unchanged.⁸ All these can cause the propagation of antibiotic-resistant micro-organisms⁹ leading to a disturbed ecosystem.

Therefore, the development of a robust, rapid and straightforward analytical protocol for screening of Norfloxacin (NFLX) and Ofloxacin (OFLX) residues in biological fluids, sewage water, edible tissues and foodstuff is highly desirable for the control of their appropriate dosage, maintaining their pharmacokinetics and avoid environmental crisis.¹⁰ Various analytical methods for this purpose have been reported in the literature including spectrophotometry,¹¹ spectrofluorimetry,¹² voltammetry,^{13,14} capillary electrophoresis,¹⁵ chemiluminescence,^{16,17} and high performance liquid chromatography (HPLC).¹⁸ Several fluorescent probes have utilized molecular imprinting chemiluminescence,¹⁹ Neodymium-modified micellar media,²⁰ carbon dots *etc.*^{21,22} Although fluorescence-based reporters provide greater intrinsic sensitivity, many of them are, however, incompatible with biological samples because of complications arising from background scattering and autofluorescence from endogenous components.²³ Trivalent lanthanide ions have long radiative lifetimes allowing background-free measurement using time-gating. They also have sharp, well-defined long-wavelength emission fingerprints²⁴ ideal for biological applications and can therefore serve as a strong sensing platform. They can be sensitized by proximate chromophores ('antennae') and may act as attractive fluorogenic (turn on) and fluorolytic (turn-off) bio-probes. This group has extensively investigated photoluminescent lanthanide cholate supramolecular hydrogels^{25–32} by utilizing their in-built hydrophobic pockets to encapsulate small organic 'antennas'. The self-assembly brings the antenna in close proximity to the acceptor lanthanide leading to energy transfer to the lanthanide ion. This strategy thus eliminates the need for the synthesis of antenna-linker-ligand type of probes to achieve lanthanide sensitization. A variety of lanthanide-luminescence based fluoroquinolone-assays^{17,33–38} have been reported in the literature. However, tedious synthesis of the probe, complex

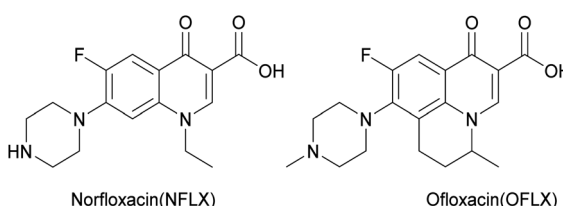


Fig. 1 Structures of Norfloxacin and Ofloxacin.

Department of Organic Chemistry, Indian Institute of Science, Bangalore, 560012, Karnataka, India. E-mail: maitra@iisc.ac.in

† Electronic supplementary information (ESI) available: Materials and methods, emission, and excitation spectra. See <https://doi.org/10.1039/d2ra03668a>



sample treatments, non-aqueous detection media, strict maintenance of pH have restricted the practical applicability of many of them.^{34–37} We have found that when doped in micromolar concentrations in Tb-Ch (5/15 mM) or Eu-Ch (5/15 mM) gels, both Norfloxacin and Ofloxacin significantly enhanced the luminescence intensities. Based on this finding we explored cholate-hydrogel based detection and quantification of these two fluoroquinolones. Initial experiments were performed in Tb (5 mM) cholate (15 mM) hydrogel by doping it with increasing concentrations of norfloxacin (NFLX). The emission intensity of Tb^{3+} showed a linear relationship with concentration (Fig. S1 in ESI†). Even 4 μM of NFLX resulted in 30-fold enhancement of sensitization of Tb^{3+} luminescence. Atomic force microscopy showed that the fibrous network of Tb^{3+} -cholate gel remained unaltered (Fig. S2 in ESI†) when NFLX was doped in micromolar concentrations, proving the robustness and stability of the sensing gel system. Fluorescence microscopic image of semi-dried NFLX doped Tb-cholate gel (Fig. S2c in ESI†) showed uniform green luminescent gel fibres, indicating that the NFLX was distributed and embedded on the hydrophobic fibres, promoting the energy transfer process making the fibres green luminescent.

In order to simplify the sensing method, we chose a paper-based system. Such sensors^{39–41} are affordable, biodegradable, sensitive, specific, user-friendly, rapid, robust, and deliverable to end-users. For this purpose, Tb-cholate (5/15 mM) gel doped with NFLX (4 μM) was prepared, sonicated for 5–6 s to reduce the viscosity, and then applied (20 μL) on a 3 mm paper disc (Fig. 2). SEM images showed dried flakes of gel on the cellulose fibre network (Fig. S3 in ESI†). The thickness of the gel layer coated on the paper surface was about 8 μm , as determined by tilt-SEM (Fig. S3c in ESI†). Time gated fluorescence (TRF) was measured on the coated discs using a plate reader. After 5 min of drying, a significantly higher Tb^{3+} luminescence output was observed, compared to that measured in wet gels (Fig. 3b, 8 vs. 7). This increase may be attributed to the efficient wicking of water molecules from the gel in the hydrophilic cellulose frameworks of paper which in turn helps reduce the OH-mediated luminescence quenching.⁴² Increased sensitization on gel-coated paper discs was observed for both NFLX and OFLX. We also confirmed that the extent of sensitization of Tb^{3+} remained constant as a function of time (Fig. S4 in ESI†). The

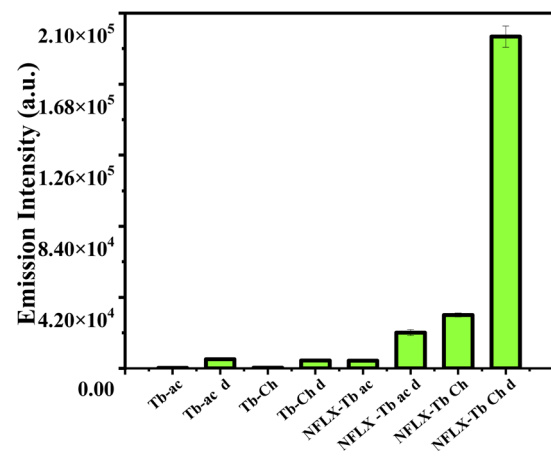


Fig. 3 Tb^{3+} -luminescence (λ_{em} 545 nm, λ_{ex} 330 nm) enhancement by NFLX (4 μM) (Ac, Ch, D: acetate solution, cholate matrix and coated paper disc, respectively).

limit of detection (LOD) for NFLX and OFLX were measured based on Tb^{3+} -luminescence output as a function of the drug concentration and were found to be 13.6 nM (Fig. S5a in ESI†) and 67 nM (Fig. S5b in ESI†), respectively. The paper-based method was used to quantify the NFLX spiked in milk samples (cow raw milk and a commercial homogenized toned milk) and in human blood serum. The LOD values measured were 68 nM, 100 nM and 100 nM, respectively (Fig. S12 and S13 in SI†). The time-gated detection method eliminated any interference from the matrix (serum or milk). This method is therefore simple, rapid, sensitive, autofluorescence and background emission free, and may thus serve as a practical tool for analytical screening.

Distinguishing two structurally similar compounds of the same class is a fundamental objective of analytical research.

Denmny *et al.* recently reported a $[\text{Ru}(\text{bpy})_3]^{2+}$ based ECL sensor⁴³ to distinguish Atropine and Scopolamine, two similar alkaloids. Encouraged by this report, we focused on the differentiation of norfloxacin and ofloxacin which have comparable 4-quinolone chromophores with similar functional groups attached (Fig. 1). With both drugs, the luminescence enhancement for Tb^{3+} was greater than that for Eu^{3+} (Fig. S8 & S9 in ESI†). Therefore, single lanthanide (Tb^{3+} or Eu^{3+}) derived gels cannot differentiate them. For this purpose, heterobimetallic ensemble strategy was explored by adopting the ratiometric detection technique.^{44,45} In order to identify optimum conditions, a set of five cholate gels samples containing varying ratios of Tb^{3+} & Eu^{3+} (maintaining total concentration of 5 mM) was prepared. This set was doped with 1 μM NFLX. An identical set was prepared with 1 μM OFLX as the dopant. After drop casting the gels on paper discs, luminescence intensities were quantified on a plate reader (Fig. 4a and b). From these data, the sensitization bias $I_{\text{Tb}}/I_{\text{Eu}}$, as measured by I_{545}/I_{617} (λ_{ex} 330 nm), was calculated and plotted against the concentration of Tb^{3+} in the mixed gel. $\text{Tb}^{3+}/\text{Eu}^{3+}$ cocktail with $[\text{Tb}^{3+}] \geq 2.5$ mM doped with NFLX showed sensitization bias (I_{545}/I_{617}) values greater than 1, whereas with OFLX the bias was always less than 1

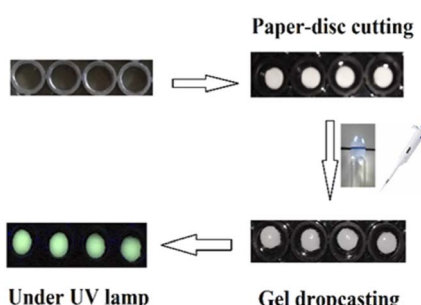


Fig. 2 Design of paper-based sensors (paper disc cutting, placing them on plate groove, gel dropcasting).

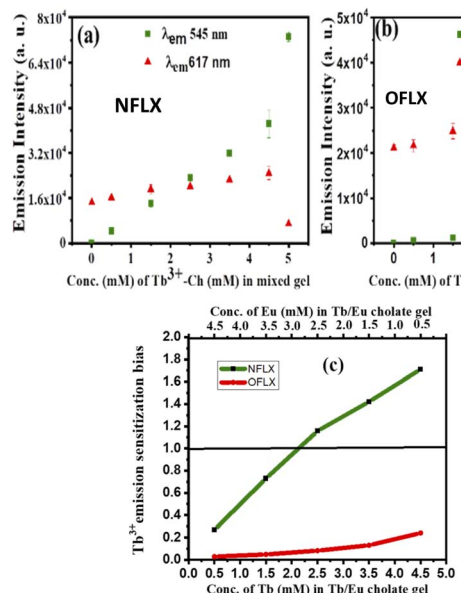


Fig. 4 Emission intensities from Tb^{3+} at 545 nm and Eu^{3+} at 617 nm ($\lambda_{\text{ex}} 330$ nm of 1 μM (a) NFLX and (b) OFLX doped mixed cholate $\{\text{[Tb}^{3+}\} + \{\text{Eu}^{3+}\} = 5 \text{ mM}\}$ gel coated discs for varying ratios of Tb^{3+} & Eu^{3+} (c) Terbium sensitization bias I_{545}/I_{617} ($\lambda_{\text{ex}} 330$ nm) as a function of Tb^{3+} concentration.

(Fig. 4c). Based on these observations we chose $\text{Tb}^{3+}/\text{Eu}^{3+}$ /cholate (4.5 mM/0.5 mM/15 mM) cocktail as the probe to differentiate these two drugs over a wider concentration range (Fig. S15 in ESI[†]). Another set of measurements were made at low μM concentrations of the drugs (Fig. S14 in ESI[†]). The Terbium sensitization bias ($I_{\text{Eu}}/I_{\text{Tb}}$) was calculated and plotted against the concentration of FLXs and found to be greater than 1 for NFLX but less than 1 for OFLX (Fig. S14c in ESI[†]). In the $\text{Tb}^{3+}/\text{Eu}^{3+}$ mixed cholate hydrogel matrix three concurrent energy transfer processes can occur—energy transfer from sensitizer (i) to Tb^{3+} , (ii) to Eu^{3+} , and (iii) energy transfer from Tb^{3+} to Eu^{3+} . While one of the emission bands of Tb^{3+} has overlap with the most intense 617 nm peak of Eu^{3+} , the Eu^{3+} emission peak at 690 nm is solely contributed by Eu^{3+} . The 690 nm emission intensity in 15 μM NFLX doped mixed gels was measured and found to linearly increase with the Tb^{3+} concentration (even though Eu^{3+} concentration is decreasing) indicating Tb^{3+} – Eu^{3+} energy transfer (Fig. S19 in ESI[†]). Significant reduction of Tb^{3+} -luminescence lifetime from 1.53 ms in NFLX doped Tb^{3+} -Ch (4.5 mM/15 mM) gel to 0.55 ms in NFLX doped $\text{Tb}^{3+}/\text{Eu}^{3+}$ -Ch (4.5 mM/0.5 mM/15 mM) gel provided additional evidence. In the $\text{Tb}^{3+}/\text{Eu}^{3+}$ /cholate (4.5 mM/0.5 mM/15 mM) cocktail, the three concurrent energy transfer processes are optimized to show $\text{Tb}^{3+}/\text{Eu}^{3+}$ emission intensity ratio exactly reversed for the two drugs (Fig. S14, S16 in ESI[†]). The optimized cocktail was subsequently used to determine the ratio of the two drugs in a mixture. The drug mixtures (total concentration 20 μM) were doped in the cocktail and the photophysical behavior was investigated. The excitation spectra corresponding to Eu^{3+} 617 nm emission showed a unique pattern depending on the ratio of NFLX and OFLX in the

mixture. The intensity (Fig. 5a) at 280 nm reflects NFLX excitation, whereas the intensity at 300 nm reflects OFLX excitation. Based on these findings, the Eu^{3+} emission intensity at 617 nm from the drug mixtures at two different excitation wavelengths 280 nm and 300 nm were evaluated. Ratiometric response $I_{617}/(I_{\text{ex} 280} + I_{\text{ex} 300})$ was found to linearly increase with the ratio of NFLX concentration to the total concentrations of both the drugs in the mixture (Fig. 5c). To validate the need for using the cocktail in this study, the excitation spectra corresponding to Eu^{3+} at 617 nm in (NFLX + OFLX) doped Eu^{3+} -Ch gel (no Tb) was recorded in which no such NFLX & OFLX ratio-dependent pattern was observed (Fig. S17 in ESI[†]). For further exploration of the cocktail, Terbium emission sensitization bias was calculated and found to be directly proportional to the ratio of NFLX concentration to the total concentrations of both the drugs in the mixture (Fig. 6b). This protocol can thus be used as a platform to determine the ratio and individual concentration of the two drugs when present in a mixture.

In conclusion, a hetero bimetallic ensemble $\text{Tb}^{3+}/\text{Eu}^{3+}$ /cholate was designed for the differentiation of structurally similar NFLX and OFLX. Till date, only physical separation by HPLC is known to quantify norfloxacin and ofloxacin concentrations in a mixture. Additionally, a paper-based sensor has also been developed for the detection and quantification of them in single drug containing system with a lower nanomolar range. The method allowed autofluorescence free detection with biological samples without the need of deproteinization and sample processing. Nonetheless, our preliminary investigations employed to utilize ratiometric bis-lanthanide strategy will serve as the foundation for the fundamental need to differentiate structurally similar molecules. Further studies to utilize this supramolecular paper-based methodology in real diagnostic fields is underway in our lab.

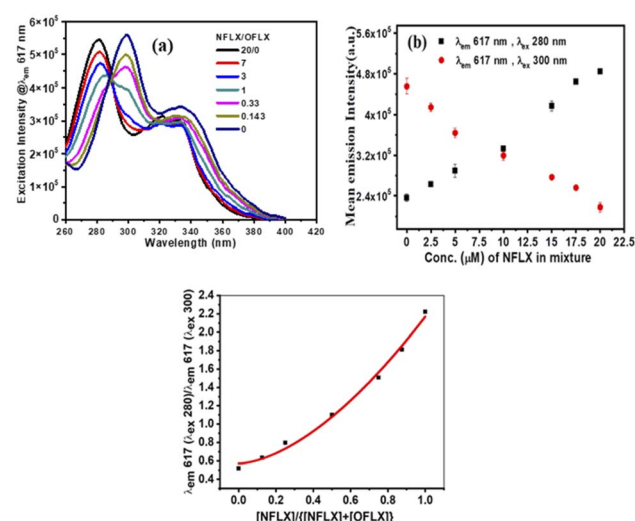


Fig. 5 (a) Excitation spectra for Eu^{3+} emission ($\lambda_{\text{em}} 617$ nm) with respect to the ratio of two drugs (b) Intensity of Eu^{3+} emission at 617 nm for two excitation wavelengths (280 nm, 300 nm) in $\text{Tb}^{3+}/\text{Eu}^{3+}$ /cholate (4.5 mM/0.5 mM/15 mM) gel coated discs with increasing concentrations of NFLX in a mixture of OFLX & NFLX, (c) intensity ratio plotted against the concentration of NFLX in the mixture.



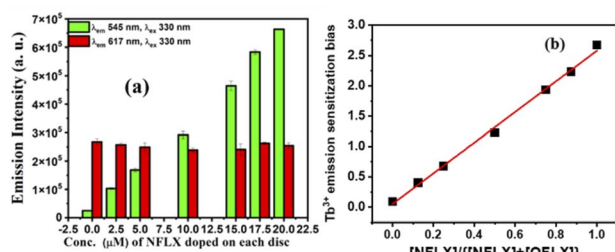


Fig. 6 (a) Tb^{3+} emission at 545 nm and Eu^{3+} emission 617 nm (b) Tb^{3+} sensitization bias in Tb^{3+} / Eu^{3+} /cholate (4.5 mM/0.5 mM/15 mM) gel coated discs with the ratio of NFLX concentration to the total drug concentration in the mixture (λ_{ex} 330 nm).

Author contributions

AB performed experiments, analysed the data, and wrote the initial draft. UM revised the final manuscript. The project was supervised by UM.

Conflicts of interest

There are no conflicts to declare.

Acknowledgements

UM thanks the SERB for the award of a J.C. Bose Fellowship (SP/S2/OC-68/2007) and for grant CRG/2020/0001140. CENSE, IISc is acknowledged for providing the SEM facility. Blood serum was collected from a volunteer by IISc Health Centre professionals as per the decision (IHEC no: 5-23012019) of Institutional Human Ethics Committee (IHEC) of IISc. AB thanks the Council of Scientific and Industrial Research (CSIR), New Delhi for the award of a research fellowship.

Notes and references

- 1 R. Feng, X. Zhang, X. Xue, Y. Xu, H. Ding, T. Yan, L. Yan and Q. Wei, *ACS Appl. Bio Mater.*, 2021, **4**, 7186–7194.
- 2 Y. Song, J. Qiao, W. Liu and L. Qi, *Anal. Bioanal. Chem.*, 2021, **413**, 979–985.
- 3 S. Kabbani, A. L. Hersh, D. J. Shapiro, K. E. Fleming-Dutra, A. T. Pavia and L. A. Hicks, *Clin. Infect. Dis.*, 2018, **67**, 134–136.
- 4 S. Sachi, J. Ferdous, M. H. Sikder and S. M. Azizul Karim Hussani, *J. Adv. Vet. Anim. Res.*, 2019, **6**, 315–332.
- 5 S. R. Raz, M. G. E. G. Bremer, W. Haasnoot and W. Norde, *Anal. Chem.*, 2009, **81**, 7743–7749.
- 6 R. Chaowana and O. Bunkoed, *Anal. Bioanal. Chem.*, 2019, **411**, 6081–6090.
- 7 H. Li, J. Yin, Y. Liu and J. Shang, *J. Agric. Food Chem.*, 2012, **60**, 1722–1727.
- 8 A. Hartmann, A. C. Alder, T. Koller and R. M. Widmer, *Environ. Toxicol. Chem.*, 1998, **17**, 377–382.
- 9 J. Cama, H. Bajaj, S. Pagliara, T. Maier, Y. Braun, M. Winterhalter and U. F. Keyser, *J. Am. Chem. Soc.*, 2015, **137**, 13836–13843.
- 10 M. J. Schneider and D. J. Donoghue, *J. Chromatogr. B.*, 2002, **780**, 83–92.
- 11 B. S. Nagaralli, J. Seetharamappa and M. B. Melwanki, *J. Pharm. Biomed. Anal.*, 2002, **29**, 859–864.
- 12 S. Wang, X. Bao, B. Gao and M. Li, *Dalton Trans.*, 2019, **48**, 8288–8296.
- 13 A. M. Santos, A. Wong, F. H. Cincotto, F. C. Moraes and O. Fatibello-Filho, *Microchim. Acta*, 2019, **186**, 148–157.
- 14 Z. Liu, M. Jin, J. Cao, J. Wang, X. Wang, G. Zhou, A. van den Berg and L. Shui, *Sens. Actuators, B*, 2018, **257**, 1065–1075.
- 15 B. Deng, C. Su and Y. Kang, *Anal. Bioanal. Chem.*, 2006, **385**, 1336–1341.
- 16 H. W. Sun, L. Q. Li and X. Y. Chen, *Anal. Bioanal. Chem.*, 2006, **384**, 1314–1319.
- 17 M. Kaczmarek and S. Lis, *Analyst*, 2011, **136**, 2592–2597.
- 18 A. H. Kamal and S. F. El-Malla, *Microchem. J.*, 2019, **150**, 104151–104158.
- 19 W. Wang, Z. Gong, S. Yang, T. Xiong, D. Wang and M. Fan, *Talanta*, 2018, **208**, 120435–120442.
- 20 R. Duan, J. Jiang, S. Liu, J. Yang, M. Qiao, Y. Shi and X. Hu, *J. Sci. Food Agric.*, 2017, **97**, 2569–2574.
- 21 M. Yang, H. Li, J. Liu, W. Kong, S. Zhao, C. Li, H. Huang, Y. Liu and Z. Kang, *J. Mater. Chem. B*, 2014, **2**, 7964–7970.
- 22 V. D. Dang, A. B. Ganganboina and R. A. Doong, *ACS Appl. Mater. Interfaces*, 2020, **12**, 32247–32258.
- 23 Y. Li, H. Wang, J. Li, J. Zheng, X. Xu and R. Yang, *Anal. Chem.*, 2011, **83**, 1268–1274.
- 24 M. C. Heffern, L. M. Matosziuk and T. J. Meade, *Chem. Rev.*, 2014, **114**, 4496–4539.
- 25 S. Banerjee, R. Kandanelli, S. Bhowmik and U. Maitra, *Soft Matter*, 2011, **7**, 8207–8215.
- 26 S. Bhowmik, S. Banerjee and U. Maitra, *Chem. Commun.*, 2010, **46**, 8642–8644.
- 27 D. Bhowmik, A. Dutta and U. Maitra, *Chem. Commun.*, 2020, **56**, 12061–12064.
- 28 T. Gorai and U. Maitra, *J. Mater. Chem. B*, 2018, **6**, 2143–2150.
- 29 T. Gorai and U. Maitra, *ACS Sens.*, 2016, **1**, 934–940.
- 30 R. Laishram and U. Maitra, *Asian J. Org. Chem.*, 2017, **6**, 1235–1239.
- 31 R. Laishram, S. Bhowmik and U. Maitra, *J. Mater. Chem. C*, 2015, **3**, 5885–5889.
- 32 S. Bhowmik, T. Gorai and U. Maitra, *J. Mater. Chem. C*, 2014, **2**, 1597–1600.
- 33 A. Rieutord, L. Vazquez, M. Soursac, P. Prognon, J. Blais, P. Bourget and G. Mahuzier, *Anal. Chim. Acta*, 1994, **290**, 215–225.
- 34 S. N. Shtykov, T. D. Smirnova, Y. G. Bylinkin, N. V. Kalashnikova and D. A. Zhemerichkin, *J. Anal. Chem.*, 2007, **62**, 136–140.
- 35 F. Yu, L. Li, F. Chen and W. Liu, *Anal. Lett.*, 2010, **43**, 357–366.
- 36 M. J. Schneider, L. Yun and S. J. Lehotay, *Food Addit. Contam. A*, 2013, **30**, 666–669.



37 H. Tan, L. Zhang, C. Ma, Y. Song, F. Xu, S. Chen and L. Wang, *ACS Appl. Mater. Interfaces*, 2013, **5**, 11791–11796.

38 S. Singha and K. H. Ahn, *Sensors*, 2016, **16**, 2065–2074.

39 M. M. Gong and D. Sinton, *Chem. Rev.*, 2017, **117**, 8447–8480.

40 S. Abbasi-Moayed, H. Golmohammadi and M. R. Hormozi-Nezhad, *Nanoscale*, 2018, **10**, 2492–2502.

41 S. Chen, Y. Song, D. Ding, Z. Ling and F. Xu, *Adv. Funct. Mater.*, 2018, **28**, 1802547–1802555.

42 K. Binnemans, *Chem. Rev.*, 2009, **109**, 4283–4374.

43 K. Brown, C. Jacquet, J. Biscay, P. Allan and L. Dennany, *Anal. Chem.*, 2020, **92**, 2216–2223.

44 Z. Dai, L. Tian, B. Song, Z. Ye, X. Liu and J. Yuan, *Anal. Chem.*, 2014, **86**, 11883–11889.

45 M. S. Tremblay, M. Halim and D. Sames, *J. Am. Chem. Soc.*, 2007, **129**, 7570–7577.

